Ultrafast Relaxation Processes of Triarylpyrylium Cations

Vidmantas Gulbinas,[‡] Dimitra Markovitsi,[†] Thomas Gustavsson,*[,†] Renata Karpicz,[‡] and Michèle Veber[§]

Institute of Physics, Gostauto St. 12, 2600 Vilnius, Lithuania, CEA/Saclay, DRECAM/SPAM, CNRS−URA 331, 91191 Gif-sur-Yvette, France, and Laboratoire de Physique des Solides, CNRS−UMR 8502, Bât. 510, Université de Paris Sud, 91405 Orsay, France

Received: November 12, 1999; In Final Form: March 6, 2000

The time evolution of the fluorescence and the photoinduced absorption spectra of four triarylpyrylium cations, differing in the number of dodecyl chains attached to the chromophore, was studied by means of femtosecond fluorescence upconversion and picosecond pump−probe absorption techniques. The dependence on solvent viscosity was also examined. The results are rationalized in terms of excited and ground-state relaxation dynamics and may be differentiated into intramolecular conformational changes and intermolecular solute−solvent contributions. The dynamic fluorescence shift is related to solvent relaxation, whereas the fluorescence intensity decay is attributed to molecular twisting acting in an intricate manner. First, the geometrical relaxation reduces rapidly the fluorescence oscillator strength, but it also greatly enhances the nonradiative $S_0 \leftarrow S_1$ internal conversion rate. Molecular back-twisting combined with vibrational relaxation in the ground state is shown to be the last and the slowest process of the reaction.

1. Introduction

Relaxation processes of molecules undergoing an important photoinduced change in their atomic charge distribution are known to be quite complex, even in the absence of photochemical reactions or interchromophore interactions.[1] The way that conformational relaxation processes depend on the solvent viscosity and the solute structure is of fundamental interest. In particular, solvent rearrangement may be associated with or control conformational modifications occurring both in the excited and the ground state. A major question is whether the solvent and the solute dynamics are coupled or if they take place independently.[2]

The triarylpyrylium cations shown in Figure 1 are good candidates for studies aiming to elucidate the above question. Calculations based on the CS−INDO-MRCI method have revealed that, in the ground state, the dihedral angle θ formed by the pyrylium core and the phenyl group at the para position is 30°;[3] a similar value (32°) was found by two-dimensional ^{1}H NMR experiments.[4] In the first excited singlet state, rotation of the dialkylaminophenyl group around the *y* axis leads to a decrease of the potential energy whose minimum corresponds to $\theta = 90°$. In the most stable configuration of both the ground and the first excited state, the two phenyl groups in the ortho position are coplanar with the pyrylium core. The $S_0 \rightarrow S_1$ Franck−Condon transition provokes a drastic change in the atomic charge distribution, the "dipole moment"[5] increasing from −1.6 to +14.2 D. A further increase up to +18.4 D is induced when the aryl group in the para position becomes perpendicular to the plane defined by the pyrylium ring and the aryl groups in the ortho position ($\theta = 90°$). Thus, the results of quantum chemistry calculations predict the formation of a TICT (twisted intramolecular charge-transfer state) state in the gas phase without an energy barrier. The solution properties of these compounds, studied by steady-state fluorescence spectroscopy and using the single photon counting technique,[3,6] six-wave mixing,[3] and Kerr ellipsometry,[7] corroborate the formation of a nonfluorescent TICT state.

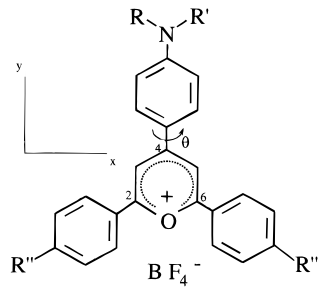

Figure 1. The studied triarylpyrylium tetrafluoroborates: P_{1-1}^+ (R = R′ = CH_3, R″ = H); P_{1-12}^+ (R = CH_3, R′ = $C_{12}H_{25}$, R″ = H); P_{12-12}^+ (R = R′ = $C_{12}H_{25}$, R″ = H); $P_{1-12(12-12)}^+$ (R= CH_3, R′=R″= $C_{12}H_{25}$).

A striking aspect regarding the excited-state relaxation of the triarylpyrylium chromophores in Figure 1 is a very strong dependence of the nonradiative decay rate on the solvent viscosity. As a matter of fact, it increases by at least 3 orders of magnitude going from ethanol to polymer matrixes. The dynamic behavior has been investigated so far only in viscous media (poly(methyl methacrylate), glycerol, ethylene glycol) with a limited time resolution.[3,7] Higher resolution experiments were necessary in order to get a better insight into the various steps of relaxation by studying its dependence on the solvent and the rotor size.

With this in mind, we have undertaken an investigation of the relaxation dynamics using femtosecond fluorescence upconversion and picosecond pump−probe absorption spectroscopy. These techniques enabled us to extend the time domain by 2 orders of magnitude with respect to previous studies, which lead us to refine the understanding of the underlying processes. We also examined a larger number of chromophores differing

* To whom correspondence should be addressed.
† CEA/Saclay, DRECAM/SPAM. E-mail: thomas@droopy.saclay.cea.fr.
‡ Institute of Physics. E-mail: vidgulb@julius.ktl.mii.lt.
§ Université de Paris Sud. E-mail: Veber@lps.u-psud.fr.

10.1021/jp9940248 CCC: $19.00
Published on Web 05/11/2000

in the number of dodecyl substituents, permitting us to discern the role of the rotor size and the solvent viscosity. The synthesis of P_{1-1}^+, P_{1-12}^+, and P_{12-12}^+ is described elsewhere,[4,6] whereas that of $P_{1-12(12-12)}^+$ is reported for the first time.

2. Experimental Details

2.1 Synthesis. The synthesis of 2,6-(4′-dodecyl)diphenyl-4-(4′-dodecylmethylaminophenyl) pyrylium tetrafluoroborate, abbreviated as $P_{1-12(12-12)}^+$, consists of the following four steps.

Synthesis of N-Dodecyl-N-Methylaniline. This compound was prepared as described in ref 6: ^{1}H NMR ($CDCl_3$, δ(ppm)): 7.2 (t, 2H); 6.65 (2 superimposed d, 3H), 3.25 (t, 2H); 2.9 (s, 3H); 1.3 (m, 20H), 0.9 (t, 3H).

Synthesis of 4-Dodecylacetophenone. This compound was prepared by a Friedel and Craft reaction, using dried CH_2Cl_2 as solvent. Acetyl chloride (4.0 mL, 0.058 mol) was added dropwise while stirring at −10 °C to a suspension of aluminum chloride (7.78 g, 0.058 mol) in dry dichloromethane (40 mL). The resulting solution was then left to stir for a further 10 minutes to allow for completion of generation of the pale yellow acetyl chloride/aluminum chloride complex. Then, 1-phenyldodecane (14.4 mL, 0.05 mol) was added dropwise during a period of 30 min while maintaining the temperature at ca. −10 °C. After complete addition, stirring was continued for 1.5 h in at a temperature the range of −5 °C to 0 °C, then for a further 3.5 h at room temperature until the reaction was finished, as judged by thin-layer chromatography (eluent: 98% heptane, 2% ethyl acetate, silica gel). The reaction mixture was then quenched, with stirring, by concentrated hydrochloric acid (25 g) and ice (50 g), left for 1 h, and extracted with dichloromethane. The organic phase was washed with 0.1 M hydrochloric acid, neutralized with saturated sodium carbonate solution, rinsed with water, and dried over phase-separating paper. Then, the solvent was removed under reduced pressure and the resulting solid recrystallized in methanol to give 4-dodecylacetophenone (11.23 g, 78%): mp = 46.8−47.3 °C (literature:[8] 48 °C); ^{1}H NMR ($CDCl_3$, δ(ppm)): 7.9 (d, 2H, J = 9 Hz); 7.25 (d, 2H, J = 9 Hz); 2.65 (t, 2H), 2.55 (s, 3H); 1.6 (m, 2H), 1.25 (s, 18H), 0.9 (t, 3H); IR (KBr pellets) ν/cm^{-1}: 3045, 2846, 1678, 1600, 1469, 1414, 1122.

Synthesis of 2,6-(4′-Dodecyl)diphenylpyrylium Tetrafluoroborate. Commercial tetrafluoroboric acid (50% w/v solution; 8.72 mL, 0.07 mol) was added dropwise to a stirred solution of acetic anhydride (4.3 mL, 0.075 mol) in glacial acetic acid (30 mL). The addition was controlled in such a way that the temperature did not rise above 25 °C (exothermic reaction). The anhydrous tetrafluoroboric acid thus generated was immediately used in the experiment.

4-Dodecylacetophenone (18.0 g, 0.0625 mol) was dissolved with stirring and warming (∼35 °C) in triethylorthoformate (104 mL, 0.625 mol). The previously prepared anhydrous tetrafluoroboric acid was then added dropwise during a period of 50 min at room temperature. The reaction mixture was left stirring overnight, and after 22 h the crude product that had precipitated was filtered off, rinsed with ether, and then recrystallized in a minimum amount of ethyl acetate to give a bright yellow powder (8.41 g, 41%): mp 135.1−136.36 °C; ^{1}H NMR ($CDCl_3$, δ-(ppm)): 9.1 (t, 1H); 8.55 (d, 2H, J = 9 Hz); 8.15 (d, 4H, J = 9 Hz); 7.45 (d, 4H, J = 9 Hz); 2.7 (t, 24H), 1.6 (m, 4H), 1.3 (s, 36H), 0.8 (t, 6H); IR (KBr pellets) ν/cm^{-1}: 2921, 2850, 1616, 1519, 1474, 1206, 1124, 1083.9; UV λ_{max}/nm (10^{-4} M in dichloromethane): 442, 332, 296, 268.

Synthesis of 2,6-(4′-Dodecyl)diphenyl-4-(4′-dodecylmethylaminophenyl)pyrylium Tetrafluoroborate. 2,6-(4′-Dodecyl)-diphenylpyrylium tetrafluoroborate (0.98 g, 1.5 × 10^{-3} mol) and *N*-dodecyl-*N*-methyl aniline (7.65 × 10^{-4} mol) were heated together while stirring under reflux in *N*,*N*-dimethylformamide (1.5 mL). The reaction mixture immediately turned to a very deep purple color. The reaction was complete after 3 h. After cooling, the reaction mixture was washed with water and extracted with dichloromethane. The organic phase was dried with phase-separating paper and the pyrylium salt precipitated with ethyl acetate. The crude product was then recrystallized in an ethanol/water mixture and extracted with heptane/CH_2Cl_2 (25/1). Finally, the desired pyrylium salt was obtained (0.16 g; 22.5%) by column chromatography (eluent: 66% CH_2Cl_2, 34% EtOAc, silica gel): ^{1}H NMR ($CDCl_3$, δ(ppm)): 8.2 (2 superimposed d and 1s, 8H); 7.5 (d, 4H, J = 9 Hz); 6.6 (d, 2H, J = 9 Hz), 3.0 (broad t poorly resolved, 5H); 2.7 (t, 4H); 1.3 (m, 60H), 0.9 (t, 9H); IR (KBr pellets); ν/cm^{-1}: 2917, 2850, 1637, 1581, 1568, 1511, 1469, 1409, 1355, 1262, 1216, 1194, 1084.

2.2 Apparatus and Procedure. Steady-state absorption and emission spectra of the solutions were recorded with a CARY 3E spectrophotometer and a SPEX Fluorolog 2F111A1 spectrofluorometer, respectively.

Solutions had an optical density between 0.5 and 1 at 394 nm for the femtosecond fluorescence measurements and about 0.3 at 527 nm for the transient absorption experiments. In both cases, the optical path length was 1 mm. The corresponding concentrations were ca. 5 × 10^{-4} M and 5 × 10^{-5} M for fluorescence and absorption experiments, respectively.

Time-resolved emission spectra and their kinetics were obtained by the fluorescence upconversion technique. The experimental setup is described in detail elsewhere.[9] The femtosecond laser source was a Ti:sapphire laser (Coherent MIRA 900) pumped by a continuous wave Ar^+ laser (Coherent INNOVA 310). The samples were excited at 394 nm by the second harmonic of the main laser radiation. After passage through a delay line, the residual fundamental was focused into a 0.2-mm BBO upconversion crystal, thus serving as the gating pulse for sum-frequency generation. The fluorescence was collected with a parabolic mirror and focused into the upconversion crystal together with the gating pulse. The upconverted light was focused onto the entrance slit of a monochromator (Jobin-Yvon HR250), and the spectrally selected upconversion light was detected by a photomultiplier connected to a lock-in photon counter. Time-resolved fluorescence spectra were recorded directly by simultaneously changing the monochromator wavelength, rotating the upconversion crystal, and changing the delay line position in order to compensate for the group velocity dispersion. The fluorescence kinetics were measured by changing only the delay line position.

The time-resolved fluorescence spectra were corrected for the spectral response of the detection system as described in ref 9. The fluorescence lifetimes were too short to record a "relaxed" fluorescence spectrum. The construction of the correction factor was therefore based on the calculated ratio between the steady-state fluorescence spectrum and the numerically time-integrated fluorescence spectrum recorded by the upconversion system. In all cases, the total intensity dropped to zero before the end of the scan. To characterize the evolution and the relaxation of the fluorescence spectrum, the corrected time-resolved spectra were fitted by log-normal functions.[10] From these fits, the total intensity (integrated in the frequency domain for a given time delay), the mean frequency, the bandwidth, and the asymmetry were obtained as functions of time.

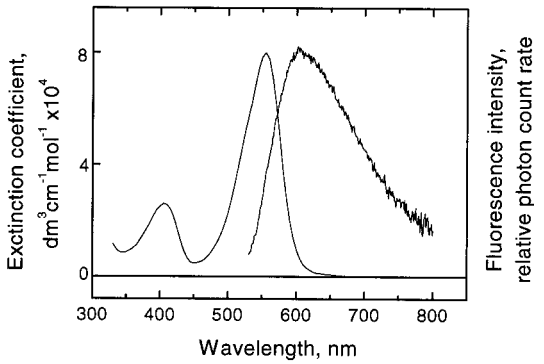

Figure 2. Steady-state absorption and fluorescence (λ_{ex} = 527 nm) spectra of $P_{1-12(12-12)}^+$ in dichloromethane.

The transient absorption study was performed using a pump−probe spectrometer equipped with a homemade low-repetition rate (1 Hz) Nd:glass laser, delivering pulses of 3 ps duration. The second harmonic (527 nm) was used for excitation, and a white light continuum generated in water was used to probe the samples. The continuum was split into two parts that passed through the sample at different positions, one overlapping with the excitation pulse, the second a few millimeters beside the first, serving as the reference. The probe and the reference pulses were focused onto the entrance slit of a small monochromator, and their intensities were measured by two photodiodes located at the exit slit. Transient absorption kinetics at a selected wavelength were measured by changing the delay time between the excitation and the probe pulses. Transient difference absorption spectra at fixed delay times were recorded by scanning the monochromator wavelength and simultaneously moving the delay line in order to compensate for the group velocity dispersion effect.

3. Results

Figure 2 shows the steady-state absorption and fluorescence spectra of $P_{1-12(12-12)}^+$ in dichloromethane. The absorption spectrum is characterized by an intense band peaking at 557 nm and a weaker one at 407 nm. The maximum of the fluorescence spectrum is located at 603 nm. The spectra of the three other compounds[3−5] are similar to those of P1-12(12-12)$^+$.

Figure 3 shows an example of the time-resolved fluorescence spectra, a few out of forty recorded for P_{1-12}^+ in hexanol. The time evolution of the total intensity and the fluorescence Stokes shift is presented in Figure 4.

Two important features can be seen: first, a rapid intensity decay, of the order of a few tens of picoseconds, and second, an even faster red shift of the fluorescence spectra. The total fluorescence intensity decay and the dynamic Stokes shift could be well approximated by single exponentials. It should be noted that the accuracy in the determination of the Stokes shift is not high, because it was impossible to record spectra corresponding to the fully relaxed configuration. Similar spectra and dynamics were obtained for P_{1-12}^+ in various solvents and also for the other three compounds in dichloromethane. The characteristic times of the dynamic Stokes shift ($\tau_{f,1}$) and the total intensity decay ($\tau_{f,2}$) observed for P_{1-12}^+ in different solvents and for the other three compounds in dichloromethane are given in Tables 1 and 2, respectively. It may be observed that both characteristic times found for P_{1-12}^+ increase with the solvent viscosity. Moreover, the fluorescence decay in dichloromethane becomes slower when the number of dodecyl substituents increases, whereas $\tau_{f,1}$ remains practically constant.

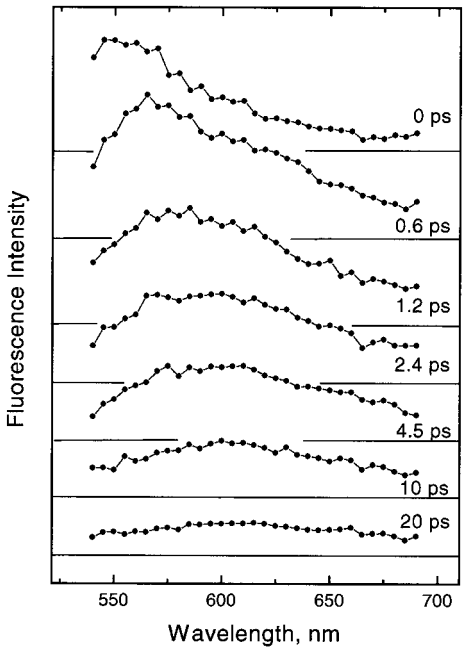

Figure 3. Corrected time-resolved fluorescence spectra of P_{1-12}^+ in hexanol; λ_{ex} = 394 nm.

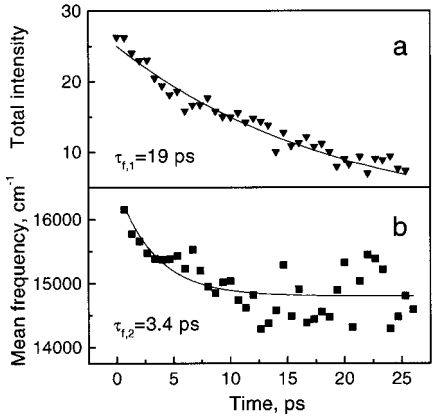

Figure 4. P_{1-12}^+ in hexanol: time dependence of (a) the total fluorescence intensity and (b) the fluorescence Stokes shift; λ_{ex} = 394 nm.

TABLE 1: Characteristic Times (ps) of the Fluorescence Stokes Shift ($\tau_{f,1}$) and the Total Intensity Decay ($\tau_{f,2}$) found for the Triarylpyrylium Cation P_{1-12}^+ in Different Solvents[a]

solvent	viscosity (cp)	$\tau_{f,1}$	$\tau_{f,2}$
dichloromethane	0.4	1.1	2.6
ethanol	1.1	1.3	4.3
dimethyl sulfoxide	2.0	1.5	6.1
hexanol	4.6	3.3	17
ethylene glycol	13.7	3.4	20

[a] Given the difficulty of locating the "relaxed" emission spectrum, we estimate the uncertainties in $\tau_{f,1}$ to ±25%. The uncertainties in $\tau_{f,2}$ are ±10%.

Figure 5 shows the differential absorption spectra of P_{1-12}^+ in hexanol recorded at different delay times after excitation. The spectra show a negative part attributed to the bleaching of the main absorption band and the stimulated emission. An induced absorption is observed around 450 and 600 nm. The induced absorption at 450 nm appears simultaneously with the bleaching, whereas the induced absorption band at 600 nm appears later.

The dynamics of the transient absorption of P_{1-12}^+ in hexanol can be seen more clearly in Figure 6. The induced absorption

TABLE 2: Characteristic Times (ps) of the Fluorescence Stokes Shift ($\tau_{f,1}$) and the Total Intensity Decay ($\tau_{f,2}$) found for the Four Studied Triarylpyrylium Cations in Dichloromethane

compound	$\tau_{f,1}$	$\tau_{f,2}$
P_{1-1}^+	0.9	1.2
P_{1-12}^+	1.1	2.6
P_{12-12}^+	1.3	3.8
$P_{1-12(12-12)}^+$	1.0	4.1

[a] Given the difficulty of locating the "relaxed" emission spectrum we estimate the uncertainties in $\tau_{f,1}$ to ±25%. The uncertainties in $\tau_{f,2}$ are ±10%.

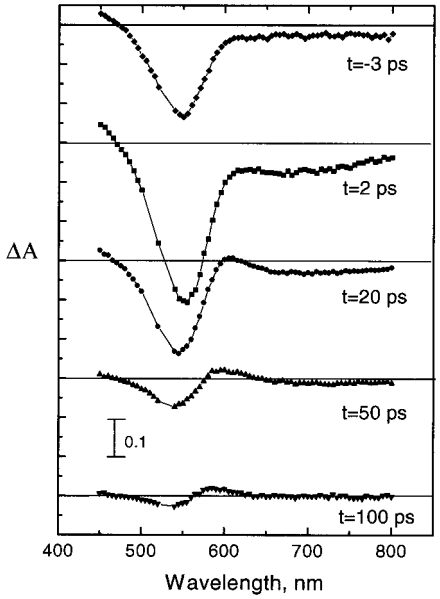

Figure 5. P_{1-12}^+ in hexanol: transient differential absorption spectra recorded at various times after excitation at 527 nm.

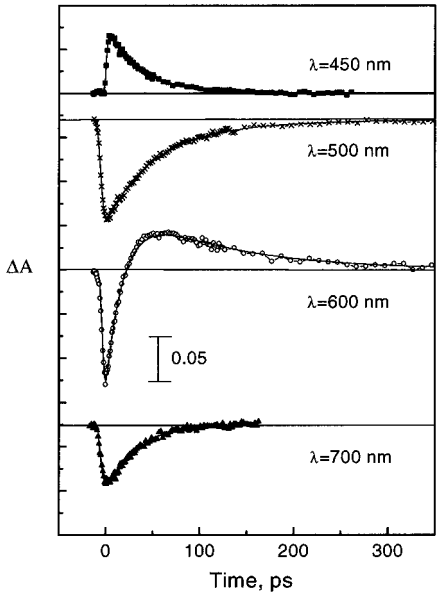

Figure 6. P_{1-12}^+ in hexanol: time dependence of the differential absorption signals observed at different wavelengths (λ_{ex} = 527 nm). The solid lines show the fit with mono- or biexponential functions convoluted with the instrumental function. The corresponding time constants and their relative amplitudes are given in Table 3.

at 450 nm and the negative differential absorbance at 500 and 700 nm decay monotonically. It is worth noticing that the decay at 500 nm is slower than those at 450 and 700 nm. The transient

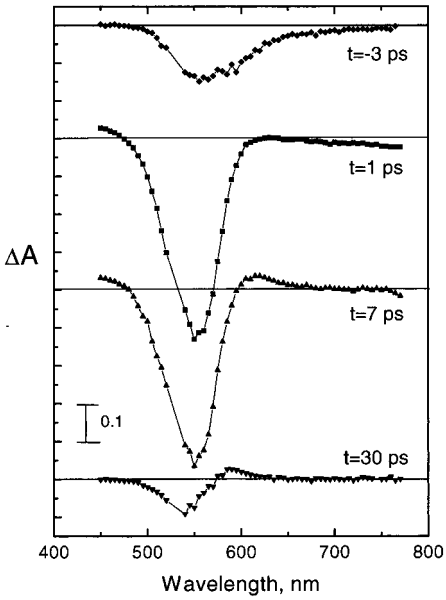

Figure 7. P_{1-1}^+ in dichloromethane: transient differential absorption spectra recorded at various delay times after excitation at 527 nm.

absorbance at 600 nm has a more complex behavior; initially it is negative, then it becomes positive and decays more slowly than the signal at 700 nm.

To compare the various decays in a quantitative way, we fitted them by the mono- or biexponential functions. Such a fit does not necessarily mean that the underlying physical process can be correctly described by such functions. The induced absorption at 450 nm decays monoexponentially with the time constant of 36 ps. The bleaching at 500 nm decays biexponentially, with 46 ps (77%) and 101 ps (23%) time constants. The induced absorption at 600 nm appears with a rise time (time needed for the signal to become positive) of 19 ps and relaxes nearly simultaneously with the minor component of the absorption bleaching. The stimulated emission at 700 nm appears with a rise time of 4.8 ps and decays faster (30 ps) than the absorption bleaching at 500 nm but slower than the total fluorescence intensity decay (17 ps).

Figure 7 shows the transient absorption spectra of P_{1-1}^+ in dichloromethane for chosen delay times. The stimulated emission around 600 nm is observed only at early times. At 1 ps delay, only the absorption bleaching and the induced absorption around 450 nm give significant contributions, whereas only a weak stimulated emission is observed at $\lambda \geq 700$ nm. The induced absorption around 600 nm appears at 7 ps delay, when the stimulated emission has already decayed.

The dynamics of the transient absorption obtained at various wavelengths for the four studied compounds in dichloromethane are shown in Figure 8. The time evolution of the absorbance is qualitatively similar to that found for P_{1-12}^+ in hexanol (Figure 6). We remark that the differential absorbance (ΔA) at all wavelengths changes more slowly with time when the number of dodecyl groups increases.

The time constants describing the signal decays observed at various wavelengths for the four studied compounds are summarized in Table 3. In most cases, monoexponential fits were satisfactory for kinetics at 450, 500, and 700 nm. The complex time dependence of the differential absorbance at 600 nm was fitted by a biexponential function. A biexponential fit was also used for the P_{1-1}^+ kinetics at 700 nm. Figure 8 illustrates how the time constants depend on the number of dodecyl groups. The decay times of the induced absorption at

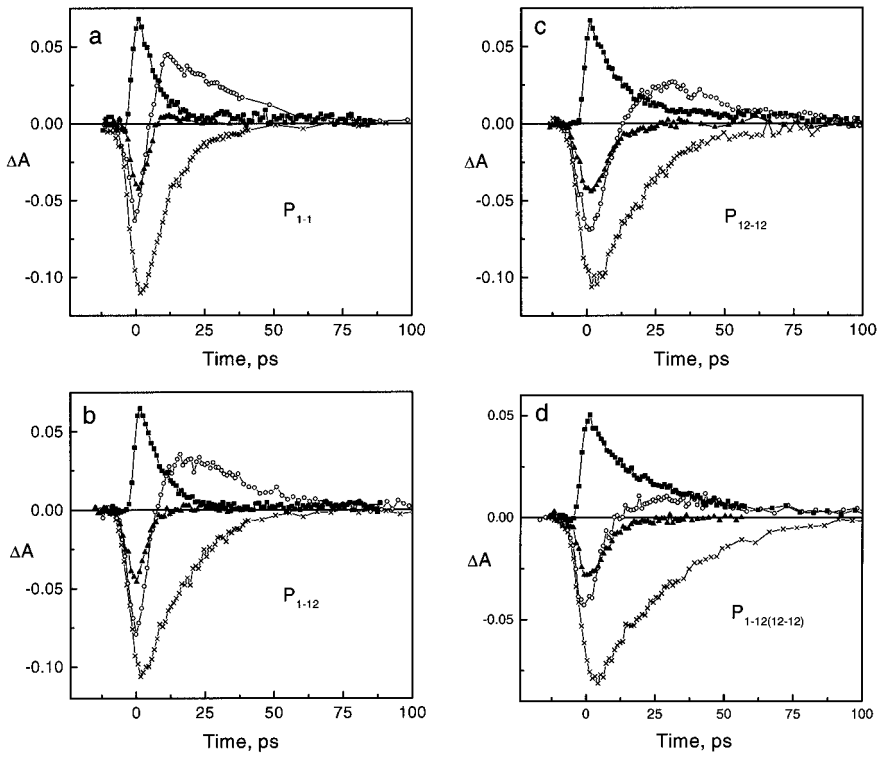

Figure 8. Time dependence of the transient absorption observed at 450 nm (squares), 500 nm (crosses), 600 nm (circles), and 700 nm (triangles) for the four studied triarylpyrylium salts in dichloromethane ($\lambda_{ex} = 527$ nm).

TABLE 3: Characteristic Times (ps) Obtained by Fitting the Transient Absorption Signals Recorded at Different Wavelengths for the Four Studied Triarylpyrylium Cations with Mono- or Biexponential Functions[a]

chromophore (solvent)	450 nm	500 nm	600 nm		700 nm
P_{1-1}^+ (dichloromethane)	5	10	3 (−100%)	24 (24%)	1
P_{1-12}^+ (dichloromethane)	6.6	16	7.2 (−100%)	23 (48%)	2.5
P_{12-12}^+ (dichloromethane)	10	20	10.4 (−100%)	28 (43%)	6.8
$P_{1-12(12-12)}^+$ (dichloromethane)	20	28	12 (−100%)	37 (21%)	6.7
P_{1-12}^+ (hexanol)	36	46 (−77%) 101 (−23%)	19 (−100%)	104 (35%)	30 4.8 (rise)

[a] The relative amplitude values are shown in parentheses.

450 nm, absorption bleaching at 500 nm, stimulated emission at 700 nm, and the rise time of the induced absorption at 600 nm increase with the number of dodecyl groups. In contrast, the decay of the induced absorption at 600 nm, which is the slowest process, shows no clear dependence.

To compare the present results to those obtained previously by Kerr ellipsometry,[7] we have explicitly studied the depolarization dynamics for P_{1-12}^+ in hexanol. Figure 9 shows the transient absorption kinetics at 500 nm for parallel ($\Delta A_{||}$) and perpendicular ($\Delta A_{\perp}$) polarization between excitation and probe pulses. Figure 9b shows the kinetics at the magic angle (54.7°) given by $\Delta A_{54.7°} = (\Delta A_{||} + 2\Delta A_{\perp})/3$ as well as the anisotropy decay given by $r = (\Delta A_{||} - \Delta A_{\perp})/(3A_0 + \Delta A_{||} + 2\Delta A_{\perp})$, where A_0 is the steady-state absorbance. We remark that the anisotropy kinetics presents a long tail (≈350 ps) component that is absent from the magic angle decay.

4. Discussion

We have seen in Section 3 (Tables 1 and 2) that the characteristic times of the dynamic Stokes shift, $\tau_{f,1}$, found for

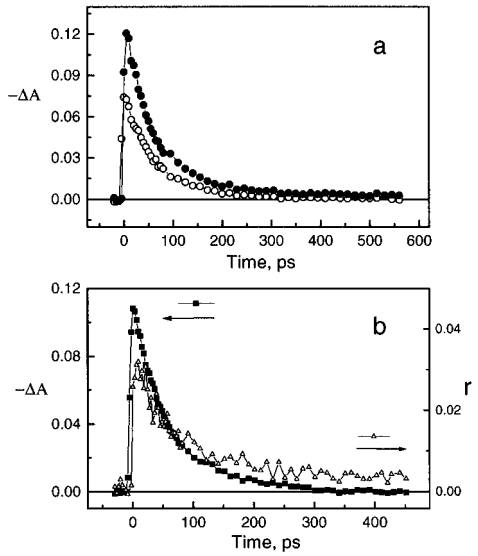

Figure 9. P_{1-12}^+ solution in hexanol: (a) transient absorption decays at 500 nm for parallel (black circles) and perpendicular (white circles) polarization between excitation and probe pulses; (b) magic angle decay (squares) and induced anisotropy decay (triangles).

the studied triarylpyrylium cations in dichloromethane do not depend strongly on the number of dodecyl groups. In contrast, they depend on the solvent and could thus be due to solvent relaxation. Regarding the characteristic time of the total fluorescence decay, $\tau_{f,2}$, it increases with both the solvent viscosity and the number of dodecyl groups. Therefore, we associate it with a conformational relaxation involving solvent hindered motion, which can be an increase of the dihedral angle θ. One may now wonder to what extent the observed Stokes shift is caused by the solvent relaxation and/or motion along the reaction coordinate. There is an indication that the molecular twisting during the fluorescence shift is negligible. According to the quantum chemical calculations, the oscillator strength

drops down with increasing twisting angle. If the spectral shift were related to the population motion along the twisting coordinate, one would expect a fast fluorescence intensity decay to occur on the same time scale as the fluorescence shift, but such a decrease is not observed. This observation leads us to attribute the fluorescence Stokes shift to the solvent relaxation. Actually, it seems that solvation and twisting take place independently, which is corroborated by the fact that both the fluorescence shift and the decay are monoexponential within the experimental accuracy. Characteristic times of solvation dynamics have been reported for coumarins in various solvents.[11] A direct comparison between these values and those in Tables 1 and 2 is, unfortunately, not possible because the fluorescence lifetimes of the studied triarylpyrylium cation are too short to follow the Stokes shift to its end.

We will now discuss the time evolution of the transient absorption spectra by focusing on four typical wavelengths, each corresponding to a particular band, as described in Section 3.

The induced absorption at 450 nm may be assigned to the first electronically excited state. As a matter of fact, such a short-wavelength transient absorption, decaying faster than the apparatus function, was already observed for P_{1-12}^+ in polymer films by nanosecond flash photolysis.[7] The decay of the transient absorption found in the present work is significantly longer than the fluorescence lifetime, which is an indication that the excited-state population is still there but is no longer fluorescent. We deduce that the $S_1 \rightarrow S_n$ absorption transition moment is less affected by the conformational changes responsible for the fluorescence decay. This could be due to the $S_1 \rightarrow S_n$ absorption transition being polarized along the x axis, making it less sensitive than the $S_0 \leftarrow S_1$ transition, which is polarized along the y axis,[3] to a change in the angle θ. Such an explanation is corroborated by the negative value of the transient dichroism at 450 nm (Figure 2 in ref 7). Thus, it is reasonable to assume that the induced absorption at 450 nm provides a better description of the excited-state population than the emission.

The negative signal observed at 700 nm is attributed to the stimulated emission. In general, it appears within the instrumental response function. However, for P_{1-12}^+ in hexanol, which is the most slowly relaxing solvent[11] used in the present study, the stimulated emission appears with a rise time of 4.8 ps. This rise time is close to the characteristic time of the dynamic Stokes shift $\tau_{f,1}$ (3.3 ps), and it can thus be attributed to solvation.

The initial negative value of the transient absorption signal at 600 nm is partly due to the ground-state bleaching and partly to the stimulated emission. This is corroborated by the steady-state spectra (Figure 2). The induced absorption at 600 nm appears with a certain delay and decays simultaneously with the bleaching. That this delay is real may be argued for by studying the transient differential absorption spectra recorded at various delay times for P_{1-1}^+ in dichloromethane, as shown in Figure 7. At 1 ps, only bleaching is observed, the induced absorption appearing first at 7 ps. That an accidental canceling between stimulated emission and induced absorption should produce the pure bleaching spectrum observed at 1 ps seems highly improbable. These considerations lead us to attribute the induced absorption to some nonrelaxed ground-state population. The fact that the rise time of the signal increases with the solvent viscosity and the number of dodecyl substituents shows that the associated process involves solvent hindered motion.

The absorption bleaching decay time observed at 500 nm corresponds to the ground-state recovery. It can be viewed as the round trip going from the Franck−Condon excited state back to the relaxed ground state, through all possible excited and ground-state relaxation processes.

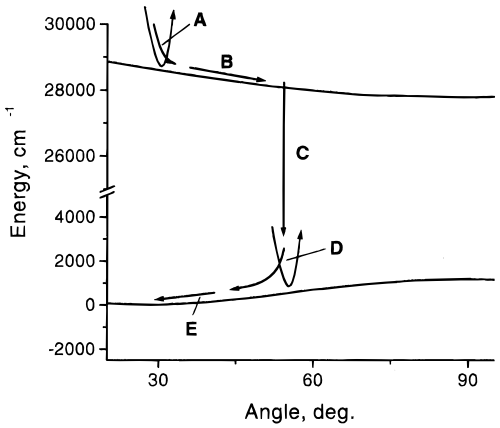

Figure 10. Schematic diagram of the excited-state relaxation of the studied triarylpyrylium tetrafluoroborates. The energy levels are those found by quantum chemistry calculations.[3] The processes marked by letters are A, solvation and population spreading; B, twisting; C, internal conversion; D, relaxation to optically active ground state; and E, ground-state relaxation.

In general, the transient absorption spectra presented here show the same behavior as the photoinduced dichroic spectra recorded by Kerr ellipsometry,[7] although the latter were obtained in more viscous solvents and with a lower time resolution. However, there is one notable exception, namely, the bleaching decay. The photoinduced dichroism at 500 nm remained long after having disappeared at 600 and 700 nm. In the present work, the bleaching decay at 500 nm is practically as fast as the 600-nm transient absorption decay (Figures 6 and 8). This discrepancy can be explained knowing that the measured parameter in Kerr ellipsometry is the dichroic angle $\delta\phi = (\Delta A_{\parallel} - \Delta A_{\perp})(\ln 10)/4$ that contains information about both population and polarization changes. Figure 9 shows that the anisotropy decay, related to the photoinduced dichroism, is much slower than the magic-angle decay. Such an effect can be provoked if the excited, initially polarized, population undergoes a depolarization before returning to the ground state. If this excited-state depolarization is faster than the depolarization of the photoinduced hole, the resulting ground-state population will be anisotropic. The exact nature of this depolarization is outside the scope of this paper.

With these observations in mind, we suggest a global scheme for the relaxation of the photoexcited triarylpyrylium cations treated in this work, as illustrated in Figure 10. The ground and excited-state free energies as functions of the dihedral angle θ are those calculated by the CS-INDO-MRCI method.[3] The characteristic times of different processes marked by letters correspond to (a) solvation and population spreading, determined from the fluorescence shift time; (b) twisting, determined from the fluorescence total intensity decay time; (c) internal conversion, determined from the induced absorption decay at 450 nm; (d) relaxation to an optically active ground state, determined from the absorption bleaching decay at 500 nm; and (e) ground-state relaxation, determined from the induced absorption decay at 600 nm. We will now discuss the different relaxation stages in detail.

After the Franck−Condon transition, the molecule finds itself on a slope of the excited-state potential curve, and its solvation shell is not equilibrated. Solvent rearrangement is the fastest process causing the fluorescence shift, as mentioned above. At the same time, the system evolves along the reaction coordinate

leading to the fast fluorescence decay. Regarding the exact origin of this fast decay, it may reflect excited-state depopulation via internal conversion to the ground state or a decrease of the fluorescence oscillator strength due to twisting. Which of the two processes is dominant at a given time depends on many factors such as the population distribution on the twisting coordinate, the population drift speed, the nonradiative decay rate, and the fluorescence oscillator strength as a function of the twisting angle. Knowing that the excited-state population decays more slowly than the fluorescence, we conclude that the fluorescence decay is largely due to the loss of the $S_0 \leftarrow S_1$ oscillator strength.

The nonradiative excited-state population continues to evolve along the twisting coordinate. The difference between the excited-state lifetime and the fluorescence decay time represents the time that molecules spend in a twisted electronically excited state. This is schematically depicted by assuming the existence of θ-intervals defined by the limiting angles θ_0 ($= 30°$), θ_1, and θ_2. In the first interval, between θ_0 and θ_1, the chromophores are fluorescent, whereas in the second interval, between θ_1 and θ_2, they are nonfluorescent. The internal conversion rate increases already for angles slightly different from θ_0, and it becomes fastest at θ_2. It is worth noticing that in solid matrixes, where twisting is inhibited, internal conversion is not efficient, as manifested by the high fluorescence quantum yield.[3] The exact dependence of the internal conversion on the twisting angle is impossible to define, but we will comment upon why it increases with θ.

An increasing internal conversion rate may be due to a decreasing transition energy as a function of θ. This energy gap dependence, which is commonly used to explain very fast internal conversion of molecules in a twisted conformation, can hardly explain the nonradiative relaxation of the studied triarylpyrylium cations. According to the calculated potential curves, the energy gap between the ground and the excited states decreases by less than 10% going from 30° to 90°. This is too small to account for an increase of the internal conversion rate by 3 orders of magnitude, as deduced from the fluorescence lifetimes measured for the chromophores in dichloromethane (Tables 1 and 2) and in solid films (3.2 ns as reported in ref 3). Even if the energy gap is insufficient to explain the data, the fast nonradiative decay may be rationalized in terms of a coordinate dependent sink.[12] In this case, one would expect a delay in the bleaching decay, as reported for 1,1-diethyl-4,4-cyanine.[13] However, no such delay has been observed for the studied triarylpyrylium cations, indicating that the internal conversion rate is substantial even for small twisting angles. In a recent paper, a similar conclusion was drawn regarding the twisting process of *N*,*N*-dimethylaminobenzylidene-1,3-indandione.[14] It was proposed that fast molecular conformational changes during the twisting time might cause the rapid internal conversion. Since the twisting mode is strongly coupled with other vibrational modes, it causes the excitation to spread over a large number of molecular vibrations. As a result, the overlap of the ground- and excited-state vibrational wave functions will increase, leading to fast internal conversion.

After internal conversion, chromophores find themselves in a nonequilibrated ground state, which we identify as responsible for the transient absorption signal observed at 600 nm. This assignment is based on the observation that the decay at 450 nm, which is a good measure of the excited-state population, is roughly similar to the rise time of the absorption at 600 nm. However, knowing that the signal at 600 nm also contains contributions from the ground-state bleaching and the stimulated emission, we cannot make a more refined comparison. In particular, we cannot determine whether the absorbing ground-state species is that formed by the $S_0 \leftarrow S_1$ Franck−Condon transition or whether it corresponds to an already partially relaxed state ($\theta_0 < \theta < \theta_2$).

The nature of the nonequilibrium ground state needs some consideration. After the internal conversion, the molecule is in a twisted ground-state configuration, it has a nonequilibrium solvation shell adapted to the excited state, and it has an excess of vibrational energy. All these effects should lead to a red shift of the absorption band. Within the framework of linear response theory,[15,16] the ground-state solvation time should be identical with that for the excited state, that is, on the order of a few picoseconds (τ_{f1} in Table 2). Thus, solvation can hardly account for signals lasting several tens of picoseconds (Figure 8). The relatively weak and nonmonotonic dependence of the induced absorption relaxation rate on the number of dodecyl groups leads us to believe that this process cannot only be due to the back-twisting. Vibrational cooling of molecules occurs at similar times of a few tens of picoseconds;[17] however, this cannot be the only process responsible for the induced absorption decay, since then no clear dependence on substituents should be observed. Moreover, the 100-ps relaxation time observed in hexanol solution is too long for cooling. We deduce that both vibrational cooling and back-twisting contribute to the ground-state relaxation. When back-twisting is very fast, vibrational cooling constitutes the limiting rate, while back-twisting becomes dominant for the larger solute molecules.

The qualitative model proposed above for the relaxation of the studied triarylpyrylium cations, involving a twist in the excited state, has been invoked in the case of many other compounds,[18,19] even if alternative explanations have been put forward.[20] We will, however, compare our findings to those reported for a particular class of molecules, namely, the triphenylmethane (TPM) dyes, because their photophysical properties are similar to those of the studied triarylpyrylium cations. After photoexcitation, TPM dyes in nonviscous solvents undergo a very rapid (on the order of a few picoseconds) internal conversion to the ground state.[12,21] A detailed account of the TPM photophysics is far outside the scope of the present work, but a very complete review article appeared recently.[22] Excited-state relaxation is explained in terms of rapid rotation of all three phenyl groups, hindered by the solvent, bringing the system to a configuration with much enhanced probability for internal conversion. After having returned to the ground state, a slower back-rotation to the equilibrium configuration takes place. The fluorescence decays much faster than the ground-state recovery. The system spends some time in a transient nonfluorescent state, as evidenced by a residual transient absorption, which is slightly red-shifted with regards to the ground-state absorption. A central question, still not resolved, is the exact nature of this transient state; is it a relaxed excited state or a nonrelaxed ground state? Several authors favor a ground-state configuration,[23] whereas recent work, based on the idea that an increase in the twist angle reduces the π-electron conjugation and thus induces a blue shift in the absorption band, opts for an excited state.[24] In the case of the studied triarylpyrylium cations, quantum chemistry calculations have shown that the $S_0 \rightarrow S_1$ transition energy of a twisted configuration ($\theta > 30°$) is lower than that for the equilibrium configuration ($\theta = 30°$).[3] This is due to the fact that, with increasing twisting angle θ, the ground state is more destabilized than the excited state. Consequently, the attribution of the 600-nm transient absorption peak to a nonequilibrated ground state is reasonable.

TABLE 4: Van der Waals Volumes (Å^3) Corresponding to the Two Rotating Parts of the Four Studied Triarylpyrylium Cations (Figure 1)[a]

chromophore	V_1	V_2	V_{TOT}	V_{RED}
P_{1-1}^+	227.8	133	360.8	84
P_{1-12}^+	227.8	320	547.8	133
P_{12-12}^+	227.8	507	734.8	157
$P_{1-12(12-12)}^+$	636.6	320	956.6	213

[a] V_1 Is the volume of the 2,6-diarylpyrylium moiety, V_2 is the volume of the 4-dialkylaminophenyl moiety, $V_{TOT} = V_1 + V_2$, and $V_{RED} = V_1 V_2/(V_1+V_2)$.

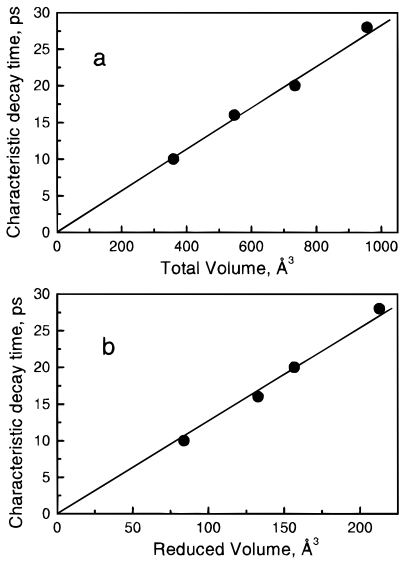

Figure 11. Characteristic times corresponding to the decay of the bleaching at 500 nm as a function of the van der Waals total (a) and reduced (b) volumes of the studied triarylpyrylium cations (Table 4).

Further comparisons between the dynamical behavior of the studied triarylpyrylium cations and the TPM dyes can be made regarding the effect of the rotor size and the influence of the solvent viscosity. We have seen in Section 3 that all time constants determined in the present work, with perhaps the exception of the dynamic Stokes shift and the 600-nm transient absorption decay, show a clear dependence on the number of the dodecyl substituents. The intramolecular rotation responsible for the observed dynamics is best described as a large amplitude motion of the two moieties of the cation, rotating with respect to each other and thus shuffling about considerable volumes of the surrounding solvent. In a very simple picture given by the Stokes−Einstein−Debye model, the rotational time, and thus the excited-state lifetime, is directly proportional to the rotor size.[25] The volumes of the two parts of the studied compounds can easily be estimated by adding up the van der Waals increments of the constituent atoms.[26] The resulting values are given in Table 4 and, as can be seen, the volumes of the two parts are comparable. For this reason, neither is a good measure of the moving volume since both will contribute to the relative motion. We will use both the total volume V_{TOT} and the reduced volume defined by $V_{RED} = V_1V_2/(V_1 + V_2)$.

Figure 11 shows that the characteristic time of the bleaching decay at 500 nm, corresponding to the overall relaxation process, is proportional to both V_{TOT} and V_{RED}. The characteristic times of the total fluorescence intensity decay, the 450-nm transient absorption decay, the 600-nm transient absorption rise, and the 700-nm stimulated emission decay also increase monotonically but not linearly with the volume. Some caution should thus be taken when interpreting the change in relaxation rate as only due to a size effect of the rotating parts. Even if this simple picture is very attractive, one should keep in mind that the dodecyl substituents cannot be considered as rigid objects, but rather as flexible, randomly curled chains. Molecular twisting, thus, may involve only parts of them. Furthermore, as noted in Section 3, the characteristic times were obtained by mono- or biexponential fits, which are not necessarily reflecting the time dependence in a correct way.

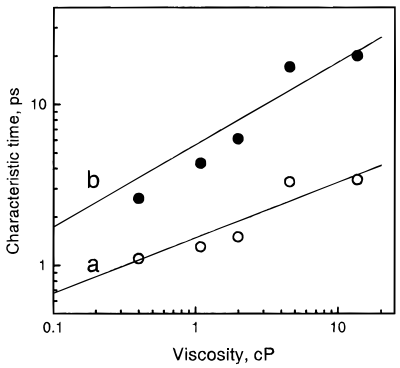

Figure 12. Characteristic times of the dynamic Stokes shift (a, open circles) and the fluorescence intensity decay (b, closed circles) of P_{1-12}^+ in dichloromethane, ethanol, dimethyl sulfoxide, hexanol, and ethylene glycol as a function of solvent viscosity. The data are fitted with the functions (a) $\tau = 1.5\eta^{0.35}$ and (b) $\tau = 5.6\eta^{0.5}$.

In our study of P_{1-12}^+ in various solvents, we observe sublinear dependencies on the solvent viscosity (η) for both the Stokes shift and the total fluorescence intensity decay (Table 1). In the former case, a $\eta^{1/3}$ dependence seems to be the case, whereas in the latter, the characteristic times are consistent with $\eta^{1/2}$ (Figure 12). A sublinear dependence on the solvent viscosity, proportional to $\eta^{2/3}$, in line with the Förster-Hoffman model,[21b] has been observed for different di- and triphenylmethane dyes.[27,28] In contrast, an exponent larger than 1 was found in a recent study of crystal violet.[24] It would therefore be very interesting to correlate these phenomenological observations to a more rational interpretation based on the electronic structure of both the solvent and the solute.

References and Notes

(1) Lippert, E.; Rettig, W.; Bonacic-Koutecky, V.; Heisel, F.; Miehé, J. A. In Prigogine, I., Rice, S. A., Eds.; Advances in Chemical Physics John Wiley & Sons: New York, 1987; Vol. 68, pp 1−173.

(2) (a) Fonseca, T.; Kim, H. J.; Hynes, J. T. *J. Mol. Liq.* **1994**, *60*, 161. (b) Fonseca, T.; Kim, H. J.; Hynes, J. T. *J. Photochem. Photobiol., A* **1994**, *82*, 67. (c) Kim, H. J.; Hynes, J. T. *J. Photochem. Photobiol., A* **1997**, *105*, 337.

(3) Markovitsi, D.; Sigal, H.; Ecoffet, C.; Millié, P.; Charra, F.; Fiorini, C.; Nunzi, J.-M.; Strzelecka, H.; Veber, M.; Jallabert, C. *Chem. Phys.* **1994**, *182*, 69.

(4) Lampre, I.; Markovitsi, D.; Birlirakis, N.; Veber, M. *Chem. Phys.* **1996**, *202*, 107.

(5) The dipole moment of a charged species, like a triarylpyrylium cation, is not coordinate-independent and needs special consideration in quantum chemistry calculations. The way these values were obtained is described in ref 3.

(6) Markovitsi, D.; Jallabert, C.; Strzelecka, H.; Veber, M. *J. Chem. Soc., Faraday Trans.* **1990**, *86*, 2819.

(7) Lampre, I.; Marguet, S.; Markovitsi, D.; Delysse, S.; Nunzi, J.-M. *Chem. Phys. Lett.* **1997**, *272*, 496.

(8) Farbenind, I. G. U.S. Patent 2,195,198, 1938.

(9) Gustavsson, T.; Cassara, L.; Gulbinas, V.; Gurzadyan, G.; Mialocq, J.-C.; Pommeret, S.; Sorgius, M.; van der Meulen, P. *J. Phys. Chem. A* **1998**, *102*, 4229.

(10) Siano, D. B.; Metzler, D. E. *J. Chem Phys.* **1969**, *51*, 1856.

(11) Horng, M. L.; Gardecki, J. A.; Papazyan, A.; Maroncelli, M. *J. Phys. Chem.* **1995**, *99*, 17311.

(12) Bagchi, B.; Fleming, G. R.; Oxtoby, D. W. *J. Chem. Phys.* **1983**, *78*, 7375.

(13) Åberg, U.; Åkesson, E.; Alvarez, J.-L.; Fedchenia, I.; Sundström, V. *Chem. Phys.* **1994**, *183*, 269.
(14) Gulbinas, V.; Kodis, G.; Jursenas, S.; Valkunas, L.; Gruodis, A.; Mialocq, J.-C.; Pommeret, S.; Gustavsson, T. *J. Phys. Chem. A* **1999**, *103*, 3969.
(15) Carter, E. A.; Hynes, J. T. *J. Chem Phys.* **1991**, *94*, 5961.
(16) Brown, R. *J. Chem Phys.* **1995**, *102*, 9059.
(17) Elsaesser, T.; Kaiser, W. *Annu. Rev. Phys. Chem.* **1991**, *42*, 83.
(18) Rettig, W. *Angew. Chem., Int. Ed. Engl*. **1986**, *25*, 971.
(19) Rettig, W. In *Topics of Current Chemistry*; Springer-Verlag: Berlin, 1994, p 254.
(20) Zachariasse, K. A.; Grobys, M.; Haar, T.; Hebecker, A.; Il'ichev, Y. V.; Jiang, Y.-B.; Morawski, O.; Kuhnle, W. *J. Photochem. Photobiol*. **1996**, *102*, 59.
(21) (a) Oster, G.; Nishijima, Y. *J. Am. Chem. Soc*. **1956**, *78*, 1581. (b) Förster, Th.; Hoffman, G. *Z. Phys. Chem. NF* **1971**, *75*, 63. (c) Cremers, C. A.; Windsor, M. W. *Chem. Phys. Lett.* **1980**, *71*, 27.
(22) Duxbury, D. F. *Chem. Rev.* **1993**, *93*, 381.
(23) Sundström, V.; Gillbro, T.; Bergström, H. *Chem. Phys.* **1982**, *73*, 439.
(24) Jurczok, M.; Plaza, P.; Martin, M. M.; Rettig, W. *J. Phys. Chem. A* **1999**, *103*, 3372.
(25) Vogel, M.; Rettig, W. *Ber. Bunsen-Ges. Phys. Chem.* **1987**, *91*, 1241.
(26) Edward, J. T. *J. Chem. Educ.* **1970**, *47*, 261.
(27) Yu, W.; Pellegrino, F.; Grant, M.; Alfano, R. R. *J. Chem. Phys.* **1977**, *67*, 1766.
(28) Hirsch, M. D.; Mahr, H. *Chem. Phys. Lett.* **1979**, *60*, 299.